

The 5th International Conference on Through-life Engineering Services (TESConf 2016)

## Advanced characterization techniques for turbine blade wear and damage

Jochen Schlobohm<sup>\*a</sup>, Oliver Bruchwald<sup>b</sup>, Wojciech Frąckowiak<sup>b</sup>, Yinan Li<sup>a</sup>, Markus Kästner<sup>a</sup>,  
Andreas Pösch<sup>a</sup>, Wilfried Reimche<sup>b</sup>, Hans Jürgen Maier<sup>b</sup>, Eduard Reithmeier<sup>a</sup>

<sup>a</sup>Institute of Measurement and Automatic Control, Nienburger Straße 17, 30167 Hannover, Germany

<sup>b</sup>Institut für Werkstoffkunde (Materials Science), An der Universität 2, 30823 Garbsen, Germany

\* Corresponding author. Tel.: +49-511-762-3236; fax: +49-511-762-3234. E-mail address: [jochen.schlobohm@imr.uni-hannover.de](mailto:jochen.schlobohm@imr.uni-hannover.de)

### Abstract

This paper presents four complementary non-destructive measurement techniques for material characterization and damage detection of turbine blades. The techniques are macroscopic fringe projection with inverse fringe projection algorithms, robot guided microscale fringe projection, high frequency eddy current and pulsed high frequency induction thermography, both in the megahertz range. The specimen on which the measurements were carried out is a blade of the 1<sup>st</sup> stage high pressure turbine of a modern airplane jet engine. The turbine blade was characterized with regard to the macroscopic and microscopic geometry, cracks in the base material as well as the condition of the protective layer system.

© 2016 The Authors. Published by Elsevier B.V. This is an open access article under the CC BY-NC-ND license (<http://creativecommons.org/licenses/by-nc-nd/4.0/>).

Peer-review under responsibility of the scientific committee of the The 5th International Conference on Through-life Engineering Services (TESConf 2016)

**Keywords:** Fringe projection; thermography; high-frequency eddy current testing; turbine blade; wear; damage;

### 1. Introduction

The reliability of jet engines is crucial for the safety of airplanes. For that reason, the performance and condition of such engines is monitored on a regular basis. The highly valuable blades of the high pressure turbine are very important for the functionality and performance of a jet engine while they are subject to high load and are exposed to extreme conditions. In order to withstand the high temperatures and severe corrosive attack, those turbine blades are protected by a corrosion protection layer (e.g. PtAl, Al or MCrAlY) and a ceramic thermal barrier coating (TBC) with a thickness of approx. 100  $\mu\text{m}$ .

This paper discusses means to non-destructively detect macroscopic defects in the turbine blade's shape, measure defects on a microscopic scale and monitor the condition of the protective layers. For the detection of geometry defects, inverse fringe projection [1] is applied. It uses a single measurement image to visualize differences of the measurement object from its nominal shape. Next, the defects found are measured and classified with a robot guided

microscale fringe projection system with a resolution of several micro meter. Defects like cracks on the surface and in the near subsurface base material as well as delamination are detected using pulsed high frequency induction thermography. Finally, high frequency eddy current testing is used to estimate the TBC thickness and to characterize the condition of the underlying corrosion protective coating. The specimen used in this study is shown in fig. 1.



Fig. 1. Image of the turbine blade tested.

### Nomenclature

HF-EC	High-Frequency Eddy Current
MRO	Maintenance, Repair and Overhaul
TBC	Thermal Barrier Coating

## 2. Inverse fringe projection

Fringe projection is an often used technique employed for measuring an object's geometry. Usually a light source, like a projector, casts light patterns onto the objects. A camera, set up at a known angle, captures those patterns. The geometry is then calculated with the triangulation principle.

For this calculation, each camera pixel is correlated with a line in the projector image (e.g. a row or column). In order to compute the correlation of camera pixels and the projector image, several sinusoidal patterns with different frequencies and phases are projected. Higher frequency patterns have a better sensitivity but make disambiguation between the periods more difficult. A pattern with one period per projector image has a relative low sensitivity but is used to identify the waves of higher frequency patterns. At least two patterns with different phases per frequency are used to reconstruct the angle of each camera pixel in the projector image. As an example, eight patterns may be used, similar to the approach of Peng [2]: 1 period ( $0^\circ$ ,  $90^\circ$ ), 6 periods ( $0^\circ$ ,  $90^\circ$ ) and 36 periods ( $0^\circ$ ,  $90^\circ$ ,  $180^\circ$ ,  $270^\circ$ ).

Inverse fringe projection is a newly developed algorithm for the detection of the deviances of an objects shape relative to the nominal geometry. The principle idea is to calculate an object adapted pattern, so that the camera captures regular and straight sinusoidal waves, if the object has no defects. The camera image of the measurement object is then compared with the ideal pattern to detect damages. The computation of the inverse pattern is done with ray tracing and a 3D model of the objects nominal geometry. In a virtual environment, the target pattern, regular sinusoidal waves, is projected from the virtual camera onto the object and captured by the virtual projector. For the measurement, the pattern captured by the virtual projector is used with the real projector and captured by the real camera.

Figure 2 shows the projected pattern and figure 3 the captured image. As expected, the fringes in the camera image are mainly regular and equidistant, which indicates that the measurement principle worked well and the blade has not been deformed too much.

Deviances in the objects geometry will cause discontinuities in the phase of the resulting image's sinusoidal pattern. The Hilbert transform [3] was used to calculate the phase of the image. Afterwards the phase image is compared with a reference phase map to create the error map (fig. 4). The reference phase map is the same as that used to calculate the inverse pattern. With a modern OpenGL graphics application the simulation can be done in about 0.1 seconds. Projection and capturing takes approximately another 0.1 seconds while the computation of the error map takes 2 seconds. The latter could be accelerated using general purpose graphic processor programming.

The cooling holes have not been part of the model used to compute the inverse pattern. Therefore, they appear as phase error in the result. Areas with a large angle between the camera and the surface normal have a high phase error because they are extremely sensitive to calibration and positioning error. The tip of the blade is heavily worn out and

hard to measure. Close to the tip are two major cracks which can be easily detected using the resulting error map.

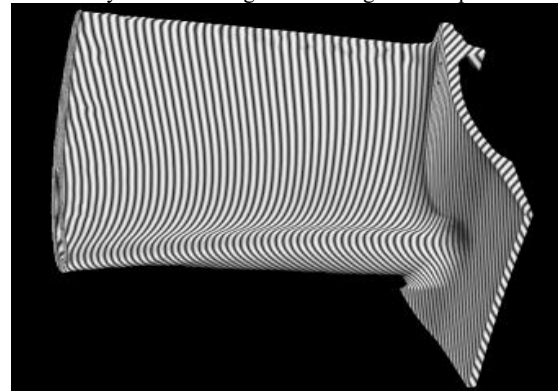


Fig. 2. Inverse pattern, projected on to the object.

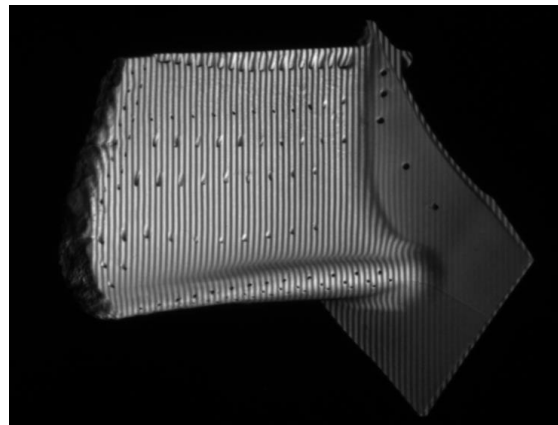


Fig. 3. Inverse pattern captured by the camera.

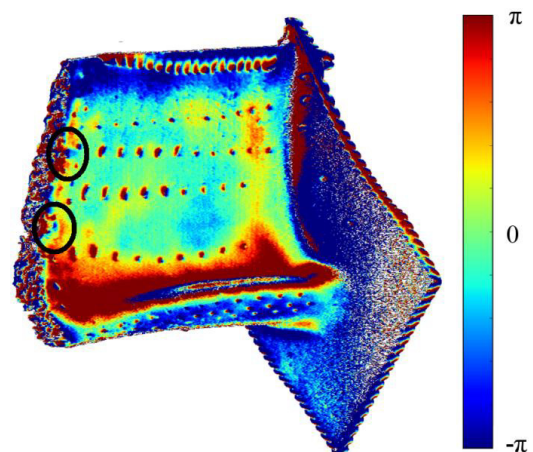


Fig. 4. Phase difference of the measured blade in radiant. Two cracks close to the tip are marked.

### 3. Microscale surface measurement

The accurate detection and evaluation of surface defects of worn turbine blades after fast geometry inspection is crucial to quality control and functional performance. In spatial surface metrology, the geometry of work pieces can be divided into different geometric scale ranges, that consist of form, waviness and roughness [4]. For the regeneration of worn turbine blades, the defect geometry varies between under 5 μm and more than 1 mm due to particles or small impacts. In this situation, the defect geometry should be measured and evaluated with high accuracy and high resolution. Micro fringe projection with a resolution of 8x8x0.3 μm<sup>3</sup> can capture details such as surface features. Due to the small measurement volume of 12x9x3 mm<sup>3</sup> of this sensor, the measurement of a complete blade requires a solution for integrating the separate measurement data into one single data set.

In this context, a robot guided microscale fringe projection system is introduced for the detection of surface defects of worn turbine blades. The combination of an industrial robot arm and a fringe projection sensor are widely used for automated optical inspection [5], [6]. In the experimental setup, the fringe projection sensor is mounted at the endeffector of the robot arm to scan the sample surface. At the same time, the position and orientation of the sensor is precisely monitored by a laser tracker to determine the six degrees of freedom (6DoF) of the sensor head.



Fig. 5 Robot guided microscale fringe projection system

Figure 5 shows the designed experimental system in our laboratory. The measurement system using the 6DoF robot kinematics requires much movement to measure and cover the complete sample surface. To reduce the moving distance, a rotation stage that carries the sample to be measured, is integrated as the additional seventh rotational axis in this measurement system. In this way, the measurement procedure can be carried out faster and the vibration influences are reduced.

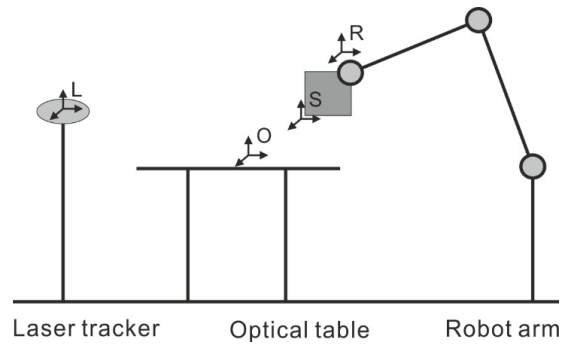


Fig. 6 Coordinate systems of the robot measurement system

To mesh the measurement data from the local coordinate system of the sensor onto a reference coordinate system, the robot guided measurement system is calibrated by a target with a known pattern. The calibration procedure can be described with the following equation:

$${}^L T_{R_i}^{-1} \cdot {}^L T_{R_{i+1}} \cdot {}^R T_S = {}^R T_S \cdot {}^S T_{O_i} \cdot {}^S T_{O_{i+1}}^{-1}$$

where  $T$  is the transformation matrix between two coordinate systems,  $L$  is the coordinate system of the laser tracker and also defined as the reference coordinate system,  $S$  is the coordinate system of the fringe projection sensor,  $R_i$  and  $O_i$  correspond to the robot endeffector coordinate system and the coordinate of object's surface at position  $i$  (see Fig. 6). Using the calibration transformation and the positioning coordinate of the laser tracker, each measurement data of a surface patch can be transformed into one single coordinate system. More details about the calibration procedure and the measurement system are given in [7], [8].

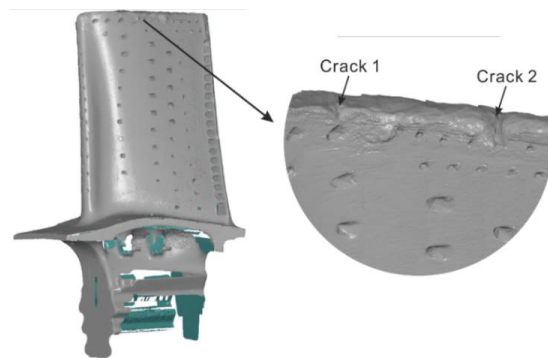


Fig. 7 High-resolution surface contour and topography of the worn turbine blade

The same worn turbine blade that was measured in the previous section was also measured with this robot guided measurement system. The left side of fig. 7 shows the complete measurement of the blade, which consists of a number of the separate surface patches. The right side shows the zoomed circle of the top of the blade, which features two small cracks. From the surface measurement, the length of the cracks can be determined as approx. 2.4 mm and approx. 3.6 mm, respectively. Additional methods for the detection and evaluation of cracks beneath the surface will be introduced in the next sections.

#### 4. Pulsed high frequency induction thermography

Induction thermography is an optical inspection technology well suited for fast and vivid detection of cracks and other thin and sharp-edged defects in electrically conductive materials. In contrast to the other optical methods using the visible spectrum of light, the induction thermography does not rely on effects such as reflection and shadowing but exploits the heat generation and heat flux as a result of actively introduced electromagnetic energy into an inspected area. The strong eddy-current field, which develops during inductive excitation, causes an increased release of heat in areas of disturbed flow due to the local rise of current density. The increase of eddy-current density and the temperature rise take place mainly at sharp edges and other narrow geometrical shape features of the specimen as well as in areas containing defects and inhomogeneities in the material. The defect information provided by the temperature distribution on the specimen's surface can be obtained and visualized using a thermal imaging system.

The fundamental parameter that determines the usability of this method and its sensitivity for defect detection is the eddy current penetration depth, which depends on the material's magnetic permeability and electrical conductivity [9]. The thin-walled turbine blades made of nickel-based superalloys with low electrical conductivity (approx. 0.6 MS/m) and low magnetic permeability ( $\mu_r \approx 1$ ) require generally high frequency excitation frequencies for damage detection. Assuming that not only the base material of the turbine blade's but also the blade's thin protective coating system should be inspected, excitation frequencies in the megahertz range are necessary to effectively generate strong eddy-currents in the near surface zone of the tested object.

Because the common transistorized high-frequency induction generators work in the kilohertz range, our set-up employs a high output generator using tube technology and excitation at frequencies between 0.1 and 3.5 MHz. An external microcontroller drives the induction generator in pulse mode. The locally introduced short-time high energy pulses improve the dynamic and sharpness in the image of the temperature field and at the same time lower the global heating of the component. Through a series of sequential excitation pulses a thermal response in the component can be generated, which results in a certain temperature-time profile for each image point. In the present study, excitation times between 50 ms and 100 ms with 50% duty cycle were found to give best results [9]. Long excitation times during the testing of metallic components lead to temperature equalization in the excited region and eventually in the whole component due to the material's thermal conductivity. Thus, the differences in the temperature field quickly vanish. Consequently, longer excitation times reduce contrast in the image between irregularities and the background and measurement sensitivity becomes lower [10, 15].

Using the excitation in the pulsed mode, the local relative temperature change is recorded. The thermal response is analyzed and filtered using a Fast-Fourier-Transform (FFT) based algorithm at every pixel of the recorded image sequence. The advantage of this approach is that the local

emissivity variation of the sample's surface, i.e. as a result of impurities, can be balanced out. Figure 8 visualizes the idea of the filtering of the infrared image sequence for extracting the damage information.

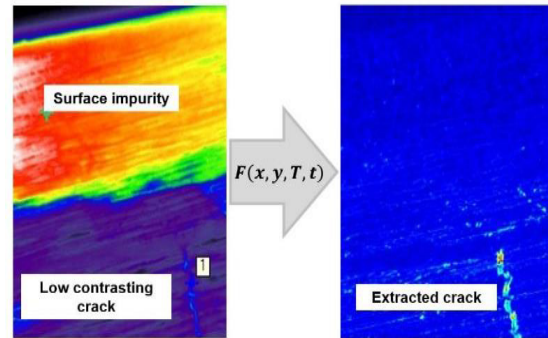


Fig. 8. Infrared image after inductive excitation of a small fragment of the blade's surface (approx. 10 cm x 7 cm) with a high emissivity area caused by a surface impurity (left). Computed IR-image with extracted damage information generated by analyzing the thermal response to the excitation (right).

Induction thermography is well suited for real-time detection of cracks and similar defects with high optical resolution at various scales. Using interchangeable lenses with different focal lengths it is possible to vary magnification and inspection times, i.e. coarse-fast / fine-slow. Moreover, the inspection can be run in fully automated mode.

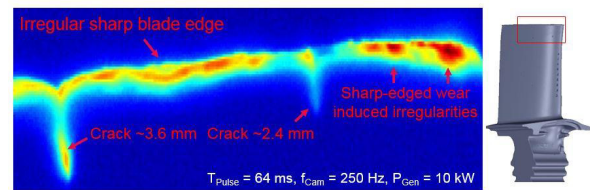


Fig. 9. Processed infrared image showing two cracks on the tip of the actual sample

For the investigation of the sample, the thermography system was equipped with a macro lens providing for a lateral resolutions of  $15\mu\text{m}$  per pixel. Figure 9 shows the computed infrared image of the magnified area at the tip of the turbine's blade with two radial cracks, which were already shown in the previous section. The resulting infrared image reveals roughly the crack contours. The presented technique of high frequency induction thermography allows distinguishing between cracks in the bulk and non-critical scratch-like surface effects avoiding false defect indications.

The experiments on other TBC coated specimens have shown that apart from crack detection in the substrate and coating material, the high frequency induction thermography can also be applied for the detection of changes in the thickness of the thermal barrier as well as debonding between the coating and the substrate.

#### 5. High frequency eddy current testing

During operation of a turbine blade, the chemical composition of the aluminium-based corrosion protective

coating (PtAl, MCrAlY) changes due to oxidation at high temperatures. Especially in the turbine blade’s highly loaded areas aluminium-oxides are formed and the amount of metallic aluminium is significantly reduced - the corrosion protective coating loses its protective function and has to be regenerated or renewed [11], [12].

Maintenance, Repair and Overhaul (MRO) companies are allowed to repair a turbine blades coating system only two or three times. Thus, there is great interest in non-destructive characterization of the coating condition prior to the repair process. Due to the fact that with the reduction of metallic aluminium the electrical conductivity of the corrosion protective coating is also characteristically reduced and therefore the electrical conductivity can be used as an indicator for the corrosion protective coatings condition. As demonstrated in the following, eddy current technology is a suitable testing method for a fast and non-destructive estimation of the coating condition.

State-of-the-art eddy current testing systems use an eddy current sensor to generate an alternating magnetic field with a typical frequency in the low single-digit MHz range. Depending on the test frequency the eddy currents can be induced in different depths of the test sample. These eddy currents generate a secondary magnetic field with a characteristic phase shift and field strength and lead to an equally characteristic, sinusoidal induced voltage in the measuring coil of the sensor. In dia- and paramagnetic materials the phase shift and amplitude of this measuring signal are based mainly on the electrical conductivity and therefore can be used to estimate the coating condition. However, due to the high eddy current penetration depth, conventional eddy current testing systems are not suitable to characterize the coating condition of the very thin corrosion protective layer separately from the base material [13], [14]. Figure 10 shows two FEM simulation results to illustrate the eddy current density and penetration depth, depending on the test frequency.

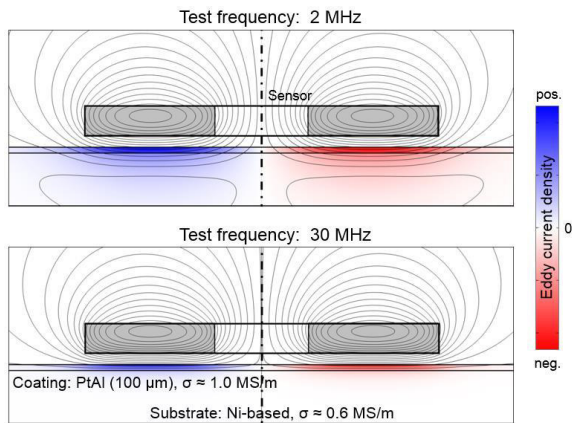


Fig. 10. FEM simulation results: Eddy current penetration depth

The simulation is based on an eddy current sensor with an outer diameter of 6 mm and a Ni-basis substrate ( $\sigma \approx 0.6 \text{ MS/m}$ ) with a  $100 \mu\text{m}$  PtAl coating ( $\sigma \approx 1.0 \text{ MS/m}$ ). As can be seen, a test frequency of approx. 30 MHz is

necessary to concentrate the majority of the eddy currents in the coating layer.

Within the framework of the CRC 871 a new HF-EC test system that operates in the frequency range up to 100 MHz and some custom-build and miniaturized sensors were developed. Due to the high test frequency, typical penetration depth of  $< 100 \mu\text{m}$  can be achieved and a separate and non-destructive characterization of the turbine blades coating condition was realized.

Figure 11 depicts the eddy current signals changes in the impedance plane while approaching the sensor towards the samples surface. The first reference measurement (grey) shows the signal for a turbine blade with a new corrosion protective coating and a non-conductive, ceramic TBC with  $100 \mu\text{m}$  thickness. Due to the fact that the distance between the sensor and the metallic material (in which the eddy current can occur) is  $\geq 100 \mu\text{m}$  - the so called Lift-Off-Effect - the signals real part is only 350 mV. However, a turbine blade with an equally new corrosion protective coating but without a TBC generates an eddy current signal with a signals real part of approximately 800 mV due to the reduced Lift-Off-Effect. Therefore the signals real part can be used to estimate the thickness of non-conductive coatings on the turbine blades surface, e.g. the TBC thickness [15].

The characteristic changes in the electrical conductivity of the corrosion protective coating that correlate with the coating

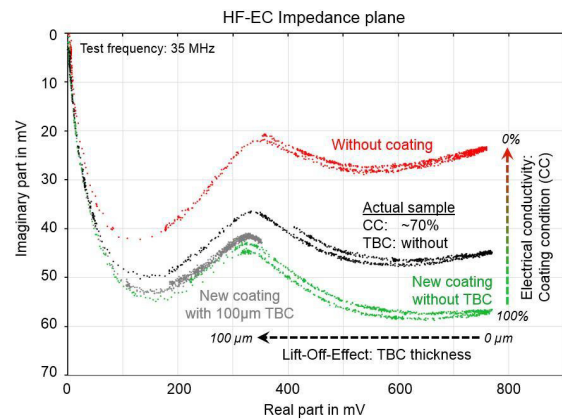


Fig. 11. Estimation of the TBC thickness and the coating condition

condition (CC) can be seen mainly in the signals imaginary part. With a new coating (green) a voltage of approximately 60 mV is obtained, whereas a consumed coating (red) with a reduced electrical conductivity leads to a reduced signals imaginary part in the range between 30 ... 20 mV. Therefore the signals imaginary part can be used to estimate the corrosion protective coatings condition [16].

The fast and reliable HF-EC measurement of the turbine blade that was examined in this paper shows no TBC and a coating condition with a value of approximately 70%.

## Conclusions

This article presents several non-destructive measurement systems with different advantages and scopes and demonstrates their application for material and wear

characterization as well as damage detection using the example of a single turbine blade. Specifically, it was shown that:

1. Deviances in the objects geometry as well as cracks can be detected by using fast inverse fringe projection.
2. Conspicuous areas can be extensively examined by means of a microscale surface measurement.
3. The pulsed high frequency induction thermography is particularly suitable for fast crack and delamination detection.
4. The TBC thickness and the condition of the underlying corrosion protective coating can be reliably estimated by using high frequency eddy current testing methods.

The combined information obtained from the different inspection systems about the geometry and material defects as well as the condition of the protective coatings may help to choose an optimal regeneration path for the turbine blades, depending on their individual condition.

### Acknowledgements

The authors thank the German Research Foundation (DFG) for funding of this study within the Collaborate Research Center (CRC) 871 regeneration of complex capital goods in the subprojects A1, A2 and C2.

### References

- [1] Pösch A, Vynnyk T, Reithmeier E. Using inverse fringe projection to speed up the detection of local and global geometry defects on free-form surfaces, Proc. SPIE 8500 (2012), DOI: 10.1117/12.928700.
- [2] Peng T. Algorithms and Models for 3-D Shape Measurement Using Digital Fringe Projections. PhD thesis (2006), University of Maryland.
- [3] Oppenheim AV, Schaffer RW. *Zeitdiskrete Signalverarbeitung*. Oldenbourg, Munich, Germany (2005).
- [4] Pfeifer T, Schmitt R. *Fertigungsmesstechnik*. Oldenbourg Verlag, 2010.
- [5] Bertagnolli F, Dillmann R. "Flexible automated process assurance through noncontact 3D measuring technology." Multisensor Fusion and Integration for Intelligent Systems, MFI2003. Proceedings of IEEE International Conference on. IEEE, 2003.
- [6] Zhang Z, et al. "Finding disaster victims: A sensory system for robot-assisted 3D mapping of urban search and rescue environments." Robotics and Automation, 2007 IEEE International Conference on. IEEE, 2007.
- [7] Krauss M, Kaestner M, Reithmeier E. Multi-Scale Inspection of Worn Surfaces for Product Regeneration in Journal of the CMSC 1/2013
- [8] Shiu YC, Shaheen A. Calibration of wrist-mounted robotic sensors by solving homogeneous transform equations of the form  $AX=XB$ , Robotics and Automation, IEEE Transactions on 5.1 (1989): 16-29.
- [9] Schlobohm J, Bruchwald O, Frackowiak W, Li Y, Kästner M, Pösch, A, et al. Turbine blade wear and damage – An overview of advanced characterization techniques, Materials Testing 58 (5), 2016, p. 389–394. DOI: 10.3139/120.110872.
- [10] Reimche W, Bernard M, Bombosch S, Scheer C, Bach Fr W. Nachweis von Anrissen in der Randzone von Hochleistungsbauteilen mit Wirbelstromtechnik und induktiv angeregter Thermographie, HTM - Journal of Heat Treatment and Materials 63(5), (2008), p. 284–297
- [11] Bräunling W. *Flugtriebwerke*. 3. Aufl., Springer-Verlag, 2009.
- [12] Cosack T. *Schutzschichten auf Turbinenschaufeln im Flugtriebwerk*, MTU Aero Engines Publikation, 2009.
- [13] Hagemäier D. Eddy current depth of penetration. Materials evaluation, 62(10), 2013, p. 1028-1029.
- [14] Campbell FC. *Inspection of metals*, ASM International, 2013
- [15] Reimche W, Bruchwald O, Frackowiak W, Bach Fr W, Maier H J. Non-Destructive Determination of Local Damage and Material Condition in High-Performance Components, HTM J. Heat Treatm. Mat 68 (2), 2009, p. 59-67, DOI: 10.3139/105.110176
- [16] Bruchwald O, Frackowiak W, Reimche W, Maier H J. Applications of high frequency eddy current technology for material characterization of thin coatings. In K. Bobzin (Eds.): *TheA Coatings 2016 Conference Proceedings*. PZH-Verlag, Garbsen, 2016, p. 37-43.